

The role of large-scale diagenesis in the formation of Vera Rubin Ridge in Gale crater, Mars, as implied by ChemCam observations. J. Frydenvang¹ (jfrydenvang@snm.ku.dk), N. Mangold², R.C. Wiens³, A.A. Fraeman⁴, L.A. Edgar⁵, C. Fedo⁶, J. L'Haridon², S. Gupta⁷, J.P. Grotzinger⁸, C. Bedford⁹, J. Bridges¹⁰, B.C. Clark¹¹, E.B. Rampe¹², O. Forni¹³, P.J. Gasda³, N.L. Lanza³, A.M. Olilla³, P.-Y. Meslin¹³, V. Payré¹⁴, F. Calef⁴, M. Salvatore¹⁵.

¹University of Copenhagen, Copenhagen, Denmark; ²LPG, Univ. de Nantes, Nantes, France; ³Los Alamos National Laboratory, Los Alamos, NM, USA; ⁴Jet Propulsion Laboratory, Pasadena, CA, USA; ⁵USGS, Flagstaff, AZ, USA; ⁶Univ. of Tennessee, Knoxville, TN, USA; ⁷Imperial College, London, UK; ⁸Caltech, Pasadena, CA, USA; ⁹Open Univ., Milton Keynes, UK; ¹⁰Univ. of Leicester, Leicester, UK; ¹¹Space Science Institute, Littleton, CO, USA; ¹²NASA Johnson Space Center, Houston, TX, USA; ¹³Institut de Recherche en Astrophysique et Planétologie, Toulouse, France; ¹⁴Rice Univ., Houston, TX, USA; ¹⁵Northern Arizona Univ., Flagstaff, AZ, USA.

Introduction: The Mars Science Laboratory (MSL) Curiosity rover has explored the Vera Rubin Ridge (VRR) in Gale crater, Mars, for more than 450 sols (Mars days) after first arriving at the ridge on sol 1800 of the mission in September 2017 (fig. 1). VRR is a topographic ridge on the central mound, Aeolis Mons (Mt. Sharp), in Gale crater that displays a strong hematite spectral signature from orbit [1]. The ridge is comprised of two stratigraphic members within the Murray formation, the Pettegrove Point member (lower) and the Jura member (upper) [2,3]. The Pettegrove Point mem-

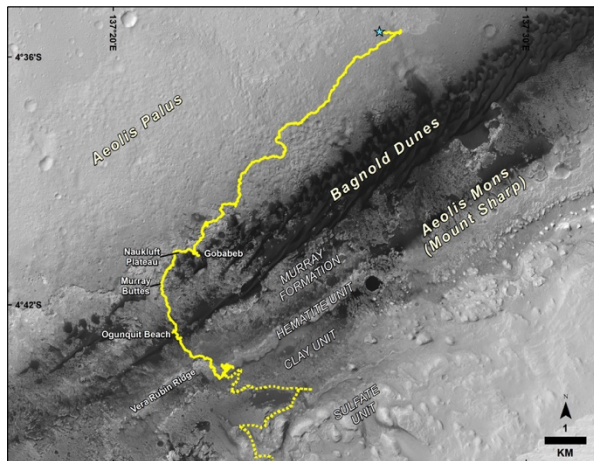


Figure 1: Curiosity's traverse from its landing site on Aeolis Palus up Mt. Sharp to its current location on Vera Rubin Ridge. The tentative future route is noted with a dashed line

ber overlies the Blunts Point member of the Murray formation [4]. The Jura member comprises bedrock showing areas of red and gray coloration. Red areas show steep ferric absorptions near 550 nm and also contain an ~860 nm absorption feature attributed to red hematite. Gray regions show weak to absent 860 nm absorption and have a weak to no ferric edge near 550 nm [5]. Generally, gray Jura rocks are found in local topographic depressions, but contacts between red and gray Jura are observed to crosscut stratigraphy [2,3]. Overall, in-situ observations show that VRR is comprised of planar-laminated mudstones similar to lithologies observed in the underlying members of the Murray formation. Sedimentary facies characteristics suggest that these

mudstones were primarily deposited in an ancient lake environment [2,3,4]. A key goal for the VRR campaign has been to characterize and understand the geochemical signature of the ridge-forming rocks to ascertain the role of primary versus diagenetic controls on the chemistry and morphology of VRR. Here, we present the results from ChemCam (*Chemistry and Camera*) instrument observations on VRR and in relation to underlying members of the Murray formation.

Methods: ChemCam measurements [6,7] enable quantification of major [8] and select minor elements [9]. Due to its speed and stand-off analysis capability, ChemCam provides the largest number of bedrock geochemistry analyses, and therefore the highest spatial resolution representation of chemical variations along Curiosity's more than 20 km traverse in Gale crater.

Our extensive rover investigations of VRR include three (N-S) traverses of the stratigraphy of VRR (fig. 2). These traverses enable an understanding of both stratigraphic and lateral geochemical variability on VRR based on the ChemCam observation points on bedrock presented here.

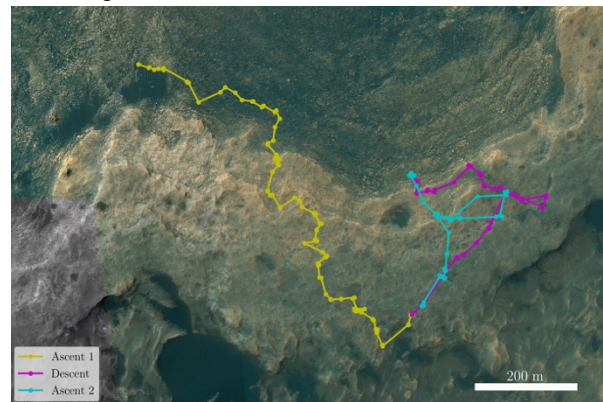


Figure 2: CCAM observation targets (points) along the three N-S traverses of the VRR stratigraphy. Lines connect targets and do not represent the route of the rover.

Results: The VRR baseline bedrock geochemistry is generally within the compositional range observed in the underlying 250+ m of Murray formation stratigraphy. Importantly, this includes the baseline bedrock iron content, which is not higher on VRR despite the

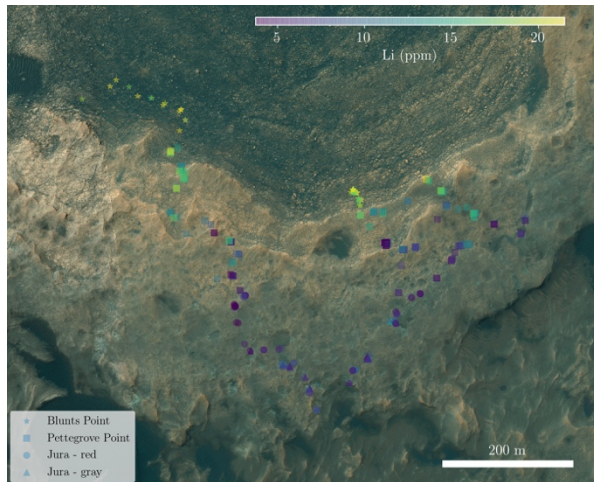


Figure 3: ChemCam bedrock observation targets on VRR. Symbols are colored according to the median Li-content of ChemCam observation points on the target. A drop in Li-content is observed up VRR (toward the bottom of the image).

strong hematite spectral signature from orbit. Evidence of apparent iron mobilization was observed on a small scale in gray Jura bedrock in the form of dark-toned high-iron concretions associated with Ca-sulfate veins, and lighter-toned areas surrounding them showing very low iron content [10,11]. While these diagenetic features (not included in figs. 3 and 4) are numerous and common in gray Jura, the baseline geochemistry of gray Jura is very similar to that of red Jura, though the MgO content tend to be slightly lower in gray Jura.

Notable chemical changes were, however, observed across the VRR stratigraphy relative to underlying Murray bedrock. Key variations include a slight decrease in Al_2O_3 and increase in K_2O . This causes the Chemical Index of Alteration (CIA) [12], which has otherwise risen up-section in the Murray formation [13], to decrease in VRR rocks. Li is also observed to decrease with elevation across the Pettegrove Point member (fig. 3). Additionally, an increase in MnO-content is observed at the contact between the Jura and Pettegrove Point members [2,3] (fig. 4).

Importantly, the multiple transects of VRR highlight that the observed geochemical variations follow the geomorphology of the modern day ridge rather than elevation (a proxy for stratigraphic position given the near horizontal dip of the Murray formation).

Discussion: In-situ observations showing that the geochemistry of VRR is generally within the range seen in the underlying Murray formation contradicts some early hypotheses on the formation of the ridge [14]. In particular, we do not see any evidence of large scale transportation and precipitation of iron on VRR. Nor do we see enrichment in immobile elements like Al and Si that would suggest that VRR is a laterite deposit.

The observed drop in Li up VRR is consistent with

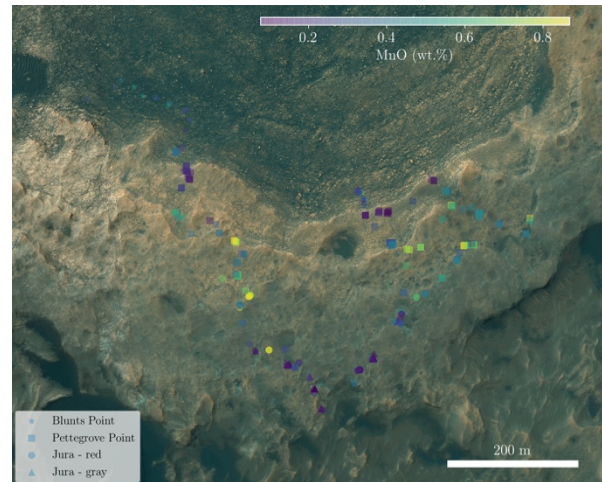


Figure 4: ChemCam bedrock observation targets on VRR. Symbols are colored according to the median MnO-content of ChemCam observation points on the target. A notable MnO enrichment is observed in the middle of VRR, and coinciding with the zone where Li is observed to decrease (fig. 3).

a drop in clay-content on VRR [15] as Li is typically found in the clay fraction [16,17]. The corresponding decrease in CIA is also consistent with a drop in clay content [18]. However, as the variations in Li and CIA do not follow stratigraphy, but rather the morphology of the ridge, our observations imply a non-stratigraphically controlled clay-content. One hypothesis to explain this is that authigenic clay formation on VRR was inhibited along a gradient that cross-cut sediment deposition.

Mn is mobilized in low pH fluids as well as reducing fluids, but the observed preferential MnO enrichment on VRR favors mobilization in a reducing fluid [19]. The co-location of the drop in Li and enrichment in MnO could be caused by the Jura member being more permeable due to lower clay content. This would enable a later reducing fluid to pass through and mobilize Mn from Jura, and deposit this at the contact to the more impermeable Pettegrove Point member.

References: [1] Fraeman A.A. et al. (2016) *JGR-P*, 121. [2] Fraeman A.A. this meeting. [3] Edgar L.A. this meeting. [4] Siebach K. this meeting. [5] Horgan B. this meeting. [6] Wiens R.C. et al. (2012), *Space Sci Rev* 170. [7] Maurice S. et al. (2012) *Space Sci Rev* 170. [8] Clegg S.M. et al., (2017) *Spectrochim. Acta B.*, 129. [9] Payré V. et al. (2017) *JGR-P*, 122. [10] L'Haridon J. et al. this meeting. [11] David G. et al. this meeting. [12] Nesbitt H.W. and Young G.M. (1984) *Geochim. et Cosmochim. Acta*, 48. [13] Mangold N. et al. (2019) *Icarus*, 321. [14] Fraeman A.A. et al. (2013) *Geology*, 41. [15] Morris R.V. this meeting. [16] Benson R.T. et al. (2017) *Nature Comm.*, 8. [17] Villumsen A. & Nielsen O.B. (1976) *Sedimentology*, 23. [18] Mischke S. & Zhang C. (2010) *Global and Planetary Change*, 72. [19] Bonatti E. et al. (1971) *Geochim. et Cosmochim Acta*, 35.